

1 **Effects of Developmental Lead and Phthalate Exposures on DNA Methylation in Adult Mouse**  
2 **Blood, Brain, and Liver Identifies Tissue- and Sex-Specific Changes with Implications for Genomic**  
3 **Imprinting**

4

5 **Rachel K. Morgan<sup>1, †</sup>, Kai Wang<sup>2, †</sup>, Laurie K. Svoboda<sup>1</sup>, Christine A. Rygiel<sup>1</sup>, Claudia Lalancette<sup>3</sup>,**  
6 **Raymond Cavalcante<sup>3</sup>, Marisa S. Bartolomei<sup>4</sup>, Rexxi Prasasya<sup>4</sup>, Kari Neier<sup>1</sup>, Bambarendage P.U.**  
7 **Perera<sup>1</sup>, Tamara R Jones<sup>1</sup>, Justin A. Colacino<sup>1,5</sup>, Maureen A. Sartor<sup>2,6</sup>, Dana C. Dolinoy<sup>1,5\*</sup>**

8 <sup>1</sup>Department of Environmental Health Sciences, School of Public Health, University of Michigan, Ann  
9 Arbor, MI 48109, USA

10 <sup>2</sup>Department of Computational Medicine and Bioinformatics, School of Medicine, University of  
11 Michigan, Ann Arbor, MI 48109, USA

12 <sup>3</sup>Epigenomics Core, School of Medicine, University of Michigan, Ann Arbor, MI 48109, USA

13 <sup>4</sup>Department of Cell and Developmental Biology, Center of Excellence in Environmental Toxicology,  
14 Perelman School of Medicine, University of Pennsylvania, Philadelphia, PA 19104, USA

15 <sup>5</sup>Department of Nutritional Sciences, School of Public Health, University of Michigan, Ann Arbor, MI  
16 48109, USA

17 <sup>6</sup>Department of Biostatistics, School of Public Health, University of Michigan, Ann Arbor, MI 48109,  
18 USA

19

20 †These authors contributed equally

21 **\*Correspondence:**

22 Dana C. Dolinoy

23 [ddolinoy@umich.edu](mailto:ddolinoy@umich.edu)

24 6671 SPH I

25 1415 Washington Heights

26 Ann Arbor, MI 48109-2029

27

28 **Conflicts of Interest**

29 *The authors declare they have nothing to disclose.*

30

## 31 Abstract

32  
33 **Background:** Maternal exposure to environmental chemicals can cause adverse health effects in  
34 offspring. Mounting evidence supports that these effects are influenced, at least in part, by epigenetic  
35 modifications.

36 **Objective:** We examined tissue- and sex-specific changes in DNA methylation (DNAm) associated with  
37 human-relevant lead (Pb) and di(2-ethylhexyl) phthalate (DEHP) exposure during perinatal development  
38 in cerebral cortex, blood, and liver.

39 **Methods:** Female mice were exposed to human relevant doses of either Pb (32ppm) via drinking water or  
40 DEHP (5 mg/kg-day) via chow for two weeks prior to mating through offspring weaning. Whole genome  
41 bisulfite sequencing (WGBS) was utilized to examine DNAm changes in offspring cortex, blood, and  
42 liver at 5 months of age. Metilene and methylSig were used to identify differentially methylated regions  
43 (DMRs). Annotatr and Chipenrich were used for genomic annotations and geneset enrichment tests of  
44 DMRs, respectively.

45 **Results:** The cortex contained the majority of DMRs associated with Pb (69%) and DEHP (58%)  
46 exposure. The cortex also contained the greatest degree of overlap in DMR signatures between sexes (n =  
47 17 and 14 DMRs with Pb and DEHP exposure, respectively) and exposure types (n = 79 and 47 DMRs in  
48 males and females, respectively). In all tissues, detected DMRs were preferentially found at genomic  
49 regions associated with gene expression regulation (e.g., CpG islands and shores, 5' UTRs, promoters,  
50 and exons). An analysis of GO terms associated with DMR-containing genes identified imprinted genes  
51 to be impacted by both Pb and DEHP exposure. Of these, *Gnas* and *Grb10* contained DMRs across  
52 tissues, sexes, and exposures. DMRs were enriched in the imprinting control regions (ICRs) of *Gnas* and  
53 *Grb10*, with 15 and 17 ICR-located DMRs across cortex, blood, and liver in each gene, respectively. The  
54 ICRs were also the location of DMRs replicated across target and surrogate tissues, suggesting epigenetic  
55 changes these regions may be potentially viable biomarkers.

56 **Conclusions:** We observed Pb- and DEHP-specific DNAm changes in cortex, blood, and liver, and the  
57 greatest degree of overlap in DMR signatures was seen between exposures followed by sex and tissue  
58 type. DNAm at imprinted control regions was altered by both Pb and DEHP, highlighting the  
59 susceptibility of genomic imprinting to these exposures during the perinatal window of development.  
60

## 61 Introduction

62 The health impacts of toxicant exposures during early life, such as lead (Pb) and phthalates (e.g., di(2-  
63 ethylhexyl) phthalate, DEHP) can be framed within the Developmental Origins of Health and Disease  
64 (DOHaD) hypothesis.<sup>1</sup> This hypothesis postulates that exposures during sensitive periods of development  
65 alter an organism's normal developmental programming, triggering a myriad of effects on growth and  
66 maturation that can persist into adulthood. Developmental exposures can impact gene expression long-  
67 term by altering the epigenome, which can have significant repercussions for health and disease.<sup>2</sup>  
68 Epigenetics refers to mitotically heritable and potentially reversible mechanisms modulating gene  
69 expression that are independent of the DNA sequence,<sup>3</sup> with the most abundantly studied mechanism  
70 being DNA methylation (DNAm). DNAm entails the addition of a methyl group to the fifth position of  
71 cytosine base adjacent to a guanine (CpG, in the majority of cases), generating what are commonly  
72 referred to as methylated cytosines (5mC), by DNA methyltransferases (DNMTs).<sup>4</sup> Increased levels of  
73 5mC within promoters and enhancers are typically associated with decreased transcription factor binding  
74 and subsequent decreases in gene expression.<sup>5</sup> Patterns of 5mC undergo waves of reprogramming (i.e.,  
75 global demethylation and remethylation) during critical windows of *in utero* development, making these  
76 periods susceptible targets of developmental exposures.<sup>6</sup>

77 Tight epigenetic regulation of imprinted genes is critical for early growth and development.<sup>7,8</sup> Imprinted  
78 genes are expressed in a mono-allelic fashion, determined in a parent-of-origin manner. For instance, a

79 paternally expressed gene will contain an active paternal allele and an inactive (e.g., methylated and thus  
80 imprinted) maternal allele. The DNAm patterns of imprinted genes expressed at specific developmental  
81 stages are important during growth and early development.<sup>9,10</sup> Once DNAm patterns have been  
82 established for these genes, often within imprinting control regions (ICRs) in gametes, they are  
83 maintained through fertilization and extensive epigenetic reprogramming events.<sup>11,12</sup> The specificity  
84 required to maintain patterns of genomic imprinting and re-establish DNAm in a parent-of-origin manner  
85 following waves of global demethylation make gestational periods particularly sensitive to environmental  
86 exposures. Environmentally-induced disruption of epigenetic processes during early development have  
87 been associated with changes in imprinted gene regulation and adverse health outcomes.<sup>13,14</sup>

88 A variety of environmental exposures, including Pb and DEHP, have been associated with altered patterns  
89 of DNAm in humans and mice.<sup>15,16</sup> Pb is a known neurotoxicant, with developmental exposures linked to  
90 neurological damage and cognition deficits in early life, as well as with increased risk of degenerative  
91 neurological disease later in life.<sup>15</sup> Although blood lead levels (BLLs) within the U.S. population have  
92 fallen dramatically, nearly 94% between 1976-1980 and 2015-2016, there is still concern regarding  
93 chronic low-levels of Pb exposure.<sup>17</sup> This is especially true for early life exposures, as the developing  
94 brain and other organ systems are particularly susceptible to the toxic effects of Pb.<sup>18</sup> Common sources of  
95 Pb exposure continue to be contaminated drinking water from leaded pipes as well as dust and chipping  
96 paint in older homes.<sup>19,20</sup> Exposure to DEHP, a phthalate commonly used as a plasticizer, has become  
97 ubiquitous, with most U.S. adults having detectable levels of DEHP metabolites in their urine.<sup>21</sup> DEHP is  
98 a known endocrine disruptor, with developmental exposures associated with altered metabolic  
99 function.<sup>16,22</sup> Common routes of DEHP exposure include personal care products, food and beverage  
100 containers, and medical equipment, making gestational and developmental exposures common.<sup>23</sup> Despite  
101 great progress over the years, gaps in knowledge remain as to whether perinatal Pb or DEHP exposure-  
102 mediated changes in DNAm have implications for long-term disease risk, whether there are sex-specific  
103 effects, and if these changes are conserved among tissues.

104 As a part of the Toxicant Exposures and Responses by Genomic and Epigenomic Regulators of  
105 Transcription (TaRGET II) Consortium,<sup>24</sup> we utilized a mouse model of human-relevant perinatal Pb and  
106 DEHP exposures to investigate genome-wide tissue- and sex-specific associations with changes in  
107 DNAm. Whole genome bisulfite sequencing (WGBS) quantified DNAm changes in blood (an easily  
108 accessible and therefore considered a “surrogate” tissue) as well as cortex and liver (two tissues often  
109 difficult to access, representing “target” tissues) collected from male and female 5-month-old mice, with  
110 and without perinatal Pb or DEHP exposures. We assessed whether perinatal Pb- or DEHP-exposed mice  
111 displayed changes in DNAm across the genome and identified imprinted genes as a relevant gene class  
112 common to these two exposures. We additionally tested whether DNAm patterns in the surrogate tissue  
113 (blood) correlated with those seen in target tissues, to determine if blood provides a viable signature for  
114 Pb- or DEHP-induced epigenetic changes in these two tissues, and how these patterns differed between  
115 males and females.

## 116 **Methods**

### 117 *Animal exposure paradigm and tissue collection*

118 Wild-type non-agouti *a/a* mice were obtained from an over 230-generation colony of viable yellow agouti  
119 (*A<sup>vy</sup>*) mice, which are genetically invariant and 93% identical to the C57BL/6J strain.<sup>25</sup> Virgin *a/a* females  
120 (6-8 weeks old) were randomly assigned to control, Pb-acetate water, or DEHP-chow two weeks prior to  
121 mating with virgin *a/a* males (7-9 weeks old). Pb- and DEHP-exposure were conducted *ad libitum* via  
122 distilled drinking water mixed with Pb-acetate or 7% corn oil chow mixed with DEHP. The Pb-acetate  
123 concentration was set as 32ppm to model human relevant perinatal exposure, where we have previously  
124 measured murine maternal BLLs around 16-60 ug/dL (mean: 32.1 ug/dL).<sup>26</sup> DEHP was dissolved in corn

125 oil from Envigo to create a customized stock solution, to produce 7% corn oil chow for experimentation.  
126 The DEHP exposure level was selected based on a target maternal dose of 5 mg/kg-day and assumes that  
127 a pregnant and nursing female mice weighs approximately 25 g and ingests roughly 5 g of chow per day.  
128 This target dose was selected as previous literature demonstrates obesity-related phenotypes in offspring  
129 exposed to 5 mg/kg-day DEHP during early development,<sup>22,27</sup> and this dosage falls within the range of  
130 exposures previously documented in humans.<sup>28</sup> All animals were maintained on a phytoestrogen-free  
131 modified AIN-93 G diet (Td.95092, 7% corn oil diet, Envigo) while housed in polycarbonate-free cages.  
132 Animal exposure to Pb or DEHP continued through gestation and lactation until weaning at post-natal day  
133 21 (PND21) when pups were switched to either Pb-free drinking water or DEHP-free chow. Perinatal  
134 exposure, thus, occurred in offspring throughout fetal development and the first three weeks after birth.  
135 Offspring were maintained until 5 months of age. This study included  $n \geq 5$  males and  $n \geq 5$  females for  
136 Pb-exposed, DEHP-exposed, and control groups, each containing 1 male and 1 female mouse per litter;  
137 and a final samples size of  $n = 108$  once tissues (i.e., cortex, blood, and liver) were collected. All animals  
138 and collected tissues were included in subsequent analyses, with no exclusions necessary. Prior to  
139 euthanasia, mice were fasted for 4 hours during the light cycle beginning in the morning, with euthanasia  
140 and tissue collection occurring in the afternoon. Immediately following mouse euthanasia with CO<sub>2</sub>  
141 asphyxiation, blood was collected through cardiac puncture, followed by dissection of the cortex and  
142 liver, which were immediately flash frozen in liquid nitrogen and stored at -80°C. Animal collection was  
143 standardized to between 1pm to 3pm and collection order was randomized daily. For each mouse, one  
144 investigator (KN) administered the treatment and was therefore aware of the treatment group allocation.  
145 All investigators completing subsequent molecular assays were blinded to treatment group, until  
146 treatment group was analyzed during bioinformatic analyses. All mouse procedures were approved by the  
147 University of Michigan Institutional Animal Care and Use Committee (IACUC), and animals were treated  
148 humanely and with respect. All experiments were conducted according to experimental procedures  
149 outlined by the NIEHS TaRGET II Consortium.<sup>24</sup> In drafting this manuscript, ARRIVE reporting  
150 guidelines were used to ensure quality and transparency of reported work.<sup>29</sup>

#### 151 *DNA extraction and whole genome bisulfite sequencing*

152 DNA extraction was performed using the AllPrep DNA/RNA/miRNA Universal Kit (Qiagen, Cat.  
153 #80224). Additional details about the animal exposures, blood collection, and blood DNA extraction can  
154 be found in previously published protocols.<sup>30</sup> Genomic DNA (gDNA) was used in the preparation of  
155 WGBS libraries at the University of Michigan Epigenomics Core. gDNA was quantified using the Qubit  
156 BR dsDNA kit (Fisher, Cat. #Q32850), and quality assessed using Agilent's Genomic DNA Tapestation  
157 Kit (Agilent, Cat. #A63880). For each sample, 200 ng of gDNA was spiked with 0.5% of unmethylated  
158 lambda DNA and sheared using a Covaris S220 (10% Duty Factor, 140W Peak Incident Power, 200  
159 Cycle/Burst, 55s). A 2 µl aliquot of processed gDNA was taken to assess shearing using an Agilent High  
160 Sensitivity D1000 Kit (Agilent, Cat. #G2991AA). Once shearing was assessed, the remaining gDNA was  
161 concentrated using a Qiagen PCR Purification column and processed for end-repair and A-tailing.  
162 Ligation of cytosine-methylated adapters was done overnight at 16°C. Following this, ligation products  
163 were cleaned using AMPure XP Beads (Fisher, Cat. #NC9933872) before processing for bisulfite  
164 conversion using the Zymo EZ DNA Methylation Kit (Zymo, Cat. #D5001), and by amplifying the  
165 bisulfite converted products over 55 cycles of 95°C for 30 seconds followed by 55°C for 15 minutes,  
166 according to the manufacturer's guidelines. After cleanup of the bisulfite converted products, final  
167 libraries were amplified over 10 cycles by PCR using KAPA Uracil+ Ready Mix (Fisher, Cat.  
168 #501965287) and NEB dual indexing primers. Final libraries were cleaned with AMPure XP beads,  
169 concentration assessed using the Qubit BR dsDNA Kit and library size assessed on the Agilent High  
170 Sensitivity D1000 Tapestation Kit. Prior to pooling, each library was quantified using KAPA Library  
171 Quantification Kit (Fisher, Cat. #501965234). We constructed four different pools of 18 libraries and each  
172 pool was sequenced on an Illumina NovaSeq6000 S4 200 cycle flow cell (PE-100) at the University of  
173 Michigan Advanced Genomics Core. Unless otherwise stated, all enzymes used in library generation were

174 purchased from New England Biolabs. Adapters with universally methylated cytosines were synthesized  
175 by Integrated DNA Technologies (IDT).

#### 176 *Data processing, quality control, and differential DNA methylation analysis*

177 FastQC<sup>31</sup> (v0.11.5) and MultiQC<sup>32</sup> (v1.8) were used to assess the quality of all sequenced samples.  
178 Sequencing adapters and low-quality bases were removed by Trim Galore<sup>33</sup> (v0.4.5). After trimming,  
179 reads shorter than 20 bp were removed from further analysis. Bismark<sup>34</sup> (v0.19.0) with Bowtie 2<sup>35</sup>  
180 (v2.3.4) as backend alignment software were used for read alignment and methylation calling with  
181 Genome Reference Consortium Mouse Build 38 (mm10) as the reference genome. All alignments were  
182 performed with 0 mismatches and multi-seed length of 20 bp. The bisulfite conversion rates were  
183 calculated through the unmethylated lambda phage DNA spike-ins. Metilene<sup>36</sup> (v0.2.8) and R  
184 Bioconductor package methylSig<sup>37</sup> (v1.4.0) were used to identify the differentially methylated regions  
185 (DMRs) independently. CpG sites with less than 10 reads or more than 500 reads were excluded from  
186 DMR detection. For methylSig, CpG sites that had reads covered in fewer than 4 samples within a  
187 treatment group were filtered out for DMR identification. Tiling windows were used with methylSig to  
188 identify DMRs, with a window size of 100 bp. For metilene, DMRs were identified *de novo* with at least  
189 5 CpGs in a single DMR. For both methods, an FDR cutoff of < 0.15 and a DNAm difference of >5%  
190 were applied to select significant DMRs. All overlapping DMRs from methylSig and metilene were  
191 confirmed to be in the same direction and merged for downstream analysis (**Supplementary Table 1**). A  
192 minimum overlap cutoff of  $\geq 10$ bp was applied to identify overlapping DMRs between tissues, sexes, and  
193 exposures, based on DMR coordinates, with no specification of methylation change direction considered  
194 for the purposes of initial comparisons. The annotatr Bioconductor package<sup>38</sup> was used to annotate all  
195 significant DMRs associated with genes and genomic locations, including CpG islands, CpG shores, CpG  
196 shelves, promoters, exons, introns, 5' UTRs, 3' UTRs, enhancers, and regions 1-5kb upstream of  
197 transcription start sites (TSSs). Random genomic regions were generated and annotated with annotatr for  
198 each tissue using the mm10 reference genome. These random regions were used as background  
199 information to show the distribution of the genomic annotation of the DMRs if distributed purely by  
200 chance. An overview of the complete methods is illustrated in **Figure 1**.

#### 201 *Geneset enrichment test*

202 R Bioconductor package Chipenrich<sup>39</sup> (v2.16.0) was used to perform gene set enrichment testing of Gene  
203 Ontology (GO) terms enriched with significant DMRs. Twelve analyses were performed stratified by  
204 each tissue and sex (i.e., male cortex, male blood, male liver, female cortex, female blood, and female  
205 liver) across each exposure group (i.e., Pb, DEHP, and control). Gene assignments were determined with  
206 the *nearest\_tss* locus definition in the *chipenrich* function to find all three categories of ontology (i.e.,  
207 Biological Process (BP), Cellular Component (CC), and Molecular Function (MF)). An FDR cutoff of <  
208 0.05 was applied for selecting significantly enriched GO terms. GO terms containing fewer than 15 genes  
209 or more than 500 genes were removed from analysis.

#### 210 *Mouse imprinted genes and imprinted control regions*

211 DMRs were compared to mouse imprinted genes and ICRs. We compiled a reference list of imprinted  
212 genes using previously documented efforts<sup>40-42</sup> and obtained ICR coordinates from Wang et al.<sup>43</sup> The valr  
213 R package<sup>44</sup> (0.6.4) was used to identify overlapping regions between the DMRs and ICRs. A Binomial  
214 test was used to assess whether the DMRs were significantly enriched in ICRs and an adjusted p-value <  
215 0.05 cutoff was utilized for identifying significant results.

## 216 **Results**

217 *Differentially methylated regions among perinatally Pb- and DEHP-exposed tissues*

218 Among Pb-exposed tissues, the majority of the DMRs were detected in the cortex (male (M) = 688,  
219 female (F) = 746), followed by blood (M = 243, F = 292), and liver (M = 100, F = 36). A similar pattern  
220 was observed in DEHP-exposed tissues, with the majority of DMRs detected in the cortex (M = 587, F =  
221 661), followed by blood (M = 312, F = 477), and liver (M = 90, F = 40) (**Figure 2A**). There was limited  
222 overlap in DMRs between each tissue type, relative to the total number detected in each tissue and sex  
223 (**Figure 2B**). For instance, Pb-exposed animals had only few DMRs appear in multiple tissues. Males had  
224 3 common DMRs among all three tissues, with 5 DMRs each overlapping between cortex and blood,  
225 between cortex and liver, and between liver and blood. Females had 7 common DMRs between cortex  
226 and blood, 3 between cortex and liver, and 1 between liver and blood, with no DMRs detected in all three  
227 tissues. Similar patterns were presented in DEHP-exposed animals, wherein males had 1 DMR common  
228 to all three tissues and 10 detected in cortex and blood, and no overlap among the remaining tissue pairs.  
229 DEHP-exposed females had more overlapping DMRs compared to males, with 2 DMR common to all  
230 tissues, 13 in both cortex and blood, 5 in cortex and liver, and 3 in liver and blood (**Figure 2B**).

231  
232 Relative to the low overlap in exposure associated DMRs between tissues, there was more DMR  
233 similarity between the sexes when stratified by tissue (**Figure 2C**), with the exception of the liver. In Pb-  
234 exposed animals, 17 and 10 DMRs were common to both males and females in the cortex and blood,  
235 respectively. Similarly, in DEHP-exposed animals, 14 and 11 DMRs were found in both males and  
236 females in the cortex and blood, respectively (**Figure 2C**). Overall, the greatest degree of DMR overlap  
237 was found between exposure types. Pb- and DEHP-exposed cortex has the greatest degree of overlap,  
238 with 79 and 47 DMRs detected under both exposure conditions in males and females, respectively  
239 (**Figure 2D**). 29 and 28 DMRs appeared in both exposure conditions in male and female blood,  
240 respectively, whereas Pb- and DEHP-exposed liver shared 2 DMRs in each sex (**Figure 2D**).

241  
242 Patterns in the direction of DNA methylation changes (DNA hyper or hypomethylation) were tissue, sex,  
243 and exposure specific (**Figure 2E**). Among Pb- and DEHP-exposed cortex, the majority of DMRs  
244 detected in males and females were hypomethylated, with slightly greater rates of hypomethylation seen  
245 in males (Pb male = 80%, Pb female = 52%, DEHP male = 60%, DEHP female = 58%). DMRs in Pb-  
246 exposed female blood, as well as DEHP-exposed male and female blood, tended to be hypermethylated  
247 (Pb female = 71%, DEHP male = 63%, DEHP female = 64%). In contrast, among Pb-exposed male  
248 blood, 56% of DMRs were hypomethylated. Patterns of directionality were more distinct between  
249 exposure types in the liver. Pb-exposed male liver presented a high proportion of hypermethylated DMRs  
250 (66%), whereas Pb-exposed female liver has slightly more hypomethylated DMRs (56%). DMR direction  
251 was roughly evenly split in DEHP-exposed liver, with 50% and 53% of DMRs hypermethylated in males  
252 and females, respectively (**Figure 2E**). **Supplementary Table 1** provides a summary of all DMRs  
253 detected in this analysis.

254  
255 *Prevalence of detected DMRs in mouse genomic regions*

256 The DMRs detected in this study occurred in specific genomic regions to a greater degree than would  
257 have been expected by a random distribution generated for comparison, given known patterns of CpG  
258 sites in the mouse genome (mm10). According to **Figure 3** and **Supplementary Table 2**, detected DMRs  
259 mapped to CpG islands to a greater degree than would have been expected by chance (3.37-19.07% of all  
260 DMRs across sex, tissues, and exposures, compared to 0.12-0.29% at random). In blood and cortex across  
261 both sexes and exposures, more DMRs were detected in 5' UTRs than predicted 4.03-8.79%, compared to  
262 0.18-0.4% under a random distribution), and a similar pattern was observed in liver of Pb-exposed males  
263 and females (2.02-2.91%) as well as DEHP-exposed females (4.8%, compared to 0.29% under a random  
264 distribution). Several transcriptional regulatory regions demonstrated significant derivation from what  
265 would be expected by chance as well. DMRs were present in promoter regions 2.83-6.61 times more than

266 would have been predicted by chance across all conditions (7.3-14.41%, compared to 1.74-2.58% at  
267 random). Exons were another notable location of DMRs, with 1.76-4.99 times more DMRs than what  
268 would have been seen under a random distribution (6.74-18.65%, compared to 3.37-3.84% at random).  
269 Conversely, there were fewer DMRs detected in the open sea (11.02-21.13% in blood, 18.40-44.94% in  
270 liver, and 19.91-25.87% in cortex) than would be expected by chance (54.56-58.09%) (**Figure 3**,  
271 **Supplementary Table 2**).

272

273 *Gene Ontology terms associated with differentially methylated region-containing genes*

274

275 DMRs were annotated using annotatr R Bioconductor package, and a summary of the overlap in DMR-  
276 containing genes across sexes, tissues, and exposures can be found in **Supplementary Figure 1**.  
277 Chipenrich was used to perform geneset enrichment tests and Gene Ontology (GO) Resource was used to  
278 identify DMR-related GO terms. The number of DMR-containing genes associated with each GO result  
279 from both Pb- and DEHP-exposed samples are summarized in **Supplementary Table 3**.  
280 Within Pb-exposed tissues, cortex had the greatest number of Gene Ontology Biological Pathway  
281 (GOBP)-related DMR-containing genes in both males (85) and females (94). DMR-associated GOBPs in  
282 female cortex were dominated by metabolic processes (35 out of 94 genes), whereas male cortex  
283 contained an abundance of DMR-containing genes related to gene expression regulation (e.g., DNA  
284 methylation or demethylation and miRNA gene silencing) (16 out of 85). The most common biological  
285 process associated with Pb exposure was genomic imprinting (GO:0071514), which appeared in male  
286 cortex, blood, and liver, as well as female cortex. In total, DMRs were detected in 21 genes associated  
287 with genomic imprinting in these tissues (**Figure 4**).

288

289 In DEHP-exposed samples, a greater number of DMR-containing genes were associated with various GO  
290 terms compared to Pb-exposed, especially the female cortex, which contained 179 genes associated with  
291 various GOBPs, most notably those associated with development (e.g., organ development,  
292 differentiation, and morphogenesis) (148 of 179). Male cortex contained far fewer GO term-associated  
293 DMRs compared to females (66 compared to 179), and there was an abundance of genes associated with  
294 gene expression regulation (10) and cellular organization (20). As with Pb-exposed tissues, the only GO  
295 term common to more than one tissue-sex combination among DEHP samples was genomic imprinting,  
296 which was associated with DMRs in 9 genes across male blood and cortex (**Figure 5**).

297

298 *DNA methylation changes at imprinted loci*

299 The appearance of imprinted genes in both exposure models during pathway analysis (**Figures 4 and 5**)  
300 was motivation to take a closer look at the effects of Pb and DEHP exposure on imprinted genes. All  
301 tissue types, across both sexes and exposures had detectable changes in DNAm within imprinted genes  
302 (**Supplementary Figures 2-5**). A reference list of imprinted genes used in this analysis can be found in  
303 **Supplemental Table 4**, and genes that did not contain a DMR in any tissue were omitted from the final  
304 figure. Cortex had the greatest number of DMRs as well as the greatest magnitude of methylation changes  
305 in assessed imprinted genes. 73 Pb-associated DMRs were detected in cortex at imprinted genes (46 in  
306 males and 27 in females with magnitude changes of 5.03-23.77%) and 67 were detected in DEHP-  
307 exposed cortex (37 in males and 30 in females with magnitude changes of 5.2-24.9%). 36 Pb-associated  
308 DMRs were detected in blood at imprinted genes (16 in males and 20 in females with magnitude changes  
309 of 5.04-20.1%) and 55 were detected in DEHP-exposed blood (32 in males and 23 in females with  
310 magnitude changes of 5.4-28.4%). Liver contained fewer changes in DNAm at imprinted genes,  
311 compared to blood and cortex, for each sex-exposure combination, with 10 DMRs in Pb-exposed liver (9  
312 in males and 1 in females with magnitude changes of 6.8-19.4%) and 11 DMRs in DEHP-exposed liver (3  
313 in males and 8 in females with magnitude changes of 8.8-16.3%). Blood from Pb-exposed females largely  
314 contained hypermethylated sites at imprinted genes (15/20 DMRs), while cortex from the same animals  
315 was largely hypomethylated in the same gene class (20/27 DMRs). A similar pattern was seen in DEHP-

316 male tissues, with the bulk of detectable changes found in the blood and cortex, with the former being  
317 largely hypermethylated (29/32 DMRs in blood) and the latter hypomethylated 23/37 DMRs in cortex)  
318 (**Supplementary Table 5**).

319 Two imprinted genes, *Gnas* and *Grb10*, contained a notable number of exposure associated DMRs. A  
320 complete overview of these DMRs is summarized in **Figure 6** and **Supplementary Table 6**. Among Pb-  
321 exposed samples, 60% and 75% of DMRs in the *Gnas* locus were hypomethylated in males and females,  
322 respectively. In Pb-exposed blood, DMRs within the *Gnas* locus were entirely hypermethylated in  
323 females (1/1) and hypomethylated in males (3/3). In Pb-exposed liver, *Gnas* DMRs were hypermethylated  
324 (2/2). Among Pb-exposed cortex, DMRs within the *Grb10* locus were largely hypermethylated in males  
325 (66%) and hypomethylated in females (66%). A similar pattern presented in Pb-exposed blood, wherein  
326 the entirety of *Grb10* DMRs in males were hypermethylated (2/2), whereas those in females were  
327 hypomethylated (1/1). Male liver contained only hypermethylated sites (2/2) within the *Grb10* locus.

328  
329 DEHP exposure was associated with more hypomethylation at the *Gnas* locus in male cortex (80%) than  
330 in females (50%). In blood, DEHP exposure associated with more hypomethylation in females (75%) but  
331 DMRs associated with this exposure in male blood were entirely hypermethylated (3/3). Regarding  
332 *Grb10*, 2/3 DMRs identified in male cortex were hypomethylated whereas 2/2 identified in male blood  
333 were hypermethylated. One hypermethylated DMR was detected in *Grb10* in DEHP-exposed female  
334 liver.

335  
336 *Exposure-associated changes in imprinting control regions*

337 Imprinted genes are regulated in part through imprinting control regions (ICRs), which are elements  
338 whose methylation is set up in the germline and that regulate gene expression and subsequent functions of  
339 imprinted gene clusters.<sup>36</sup> Changes in the DNAm status of these regions can impact the expression of  
340 imprinted and non-imprinted genes within a given cluster, thus magnifying the regulatory effects of what  
341 would otherwise be a single-gene effect.<sup>37</sup> *Gnas* contains two ICRs, the *Gnas* ICR and the *Nespas* ICR,  
342 while *Grb10* contains one ICR.<sup>36,38</sup> The current analysis identified multiple DMRs within the ICRs of  
343 both *Gnas* (7 in ICR *Gnas* and 8 in ICR *Nespas*) and *Grb10* (17 in the *Grb10* ICR) across exposure and  
344 tissue types (**Figure 7**). A binomial test was conducted to assess whether exposure-associated DMRs  
345 occurred in these ICRs to a greater degree than would have been expected by random change. Both the  
346 *Gnas* and *Grb10* ICRs contained more DMRs than would have been expected by chance in multiple sex-  
347 exposure-tissue combinations. A summary of these findings can be found in **Supplementary Table 6**.

348  
349 Pb exposure was associated with relatively limited changes in DNAm in *Gnas* ICRs when compared to  
350 *Grb10*. In the *Nespas* ICR, Pb exposure was associated with hypermethylation in female cortex (1/1  
351 DMR) and a mix of hyper- (1/2 DMRs) and hypomethylation (1/2 DMRs) in male cortex. In the *Gnas*  
352 ICR, Pb exposure was associated only with hypermethylation in male liver (1/1 DMR) (**Figure 7A** and  
353 **Supplementary Table 7**). In the *Grb10* ICR, Pb exposure was associated again with an equal amount of  
354 hyper- (3/6) and hypomethylated (3/6) DMRs, in both male and female cortex. Pb exposure was entirely  
355 associated with hypermethylation in both male blood (2/2 DMRs) and liver (2/2 DMRs) but was  
356 associated with hypomethylation in female blood (1/1 DMR) (**Figure 7B** and **Supplementary Table 7**).

357  
358 There were comparatively more changes in DNAm in the *Gnas* ICRs associated with DEHP exposure. In  
359 male cortex there was again a mix of hyper- (1/2) and hypomethylated (1/2) DMRs in the *Nespas* ICR.  
360 Unlike Pb exposure, DEHP was associated only with hypomethylated DMRs (2/2) in female cortex in the  
361 *Nespas* ICR. In male blood there was 1 and 2 hypermethylated DEHP-associated DMRs within the  
362 *Nespas* and *Gnas* ICRs, respectively. Female cortex and blood both contained a mix of hyper- (1/2) and  
363 hypomethylated (1/2) DMRs in the *Gnas* ICR associated with DEHP exposure (**Figure 7A** and  
364 **Supplementary Table 8**). Within the *Grb10* ICR, DEHP exposure was associated with a mix of hyper-



365 (1/3) and hypomethylated (2/3) DMRs in male cortex, hypermethylated (2/2) DMRs in male blood, and 1  
366 hypermethylated DMR in female liver (**Figure 7B** and **Supplementary Table 8**).

367

## 368 **Discussion**

369 Toxicant exposures that occur during critical periods of development can have ramifications for health  
370 and well-being throughout the life-course.<sup>45</sup> Perinatal Pb and DEHP exposures have been linked to  
371 aberrant brain development and metabolic function, respectively, at environmentally relevant doses.<sup>46,47</sup>  
372 With regard to epigenetic mechanisms governing gene expression, Pb and DEHP exposures have both  
373 been associated with differential DNAm in human populations.<sup>48,49</sup> Concurrently, it is unknown if  
374 toxicant-induced changes in difficult-to-access tissues, such as brain and liver, are reflected in more easily  
375 accessible (surrogate) tissues, such as blood. It is therefore pertinent to examine how two prominent  
376 developmental exposures, Pb and DEHP, affect gene regulation by DNAm in these target and surrogate  
377 tissues in order to assess whether DNAm could be used as a potential biomarker of changes in more  
378 difficult to access tissues, as is being evaluated in the TaRGET II Consortium.<sup>24</sup>

379 *Pb and DEHP Exposures are Associated with Sex, Tissue, and Exposure-Specific General Changes in*  
380 *DNA Methylation.* Overall, Pb and DEHP exposures resulted in similar number of DMRs between the  
381 sexes for each of the three tissues assessed (**Figure 2A**). The cortex contained the greatest number of  
382 DMRs for each exposure, followed by blood and liver. Between the sexes, females had more DMRs  
383 across both exposures in cortex and blood, while males had more DMRs in the liver (**Figure 2A**). This  
384 overall DNAm pattern is consistent with previous reports, which showed significant changes in DNAm in  
385 female brain following gestational Pb exposure as well as in male liver following DEHP exposure.<sup>50,51</sup>  
386 There was minimal overlap in DMRs between either cortex-blood (0.5-1.2% of total DMRs detected in  
387 these tissues) or liver-blood (0.25-1.5% of total DMRs detected in these tissues) (**Figure 2B**). The largest  
388 degree in DMR similarity between target-surrogate tissues was in DEHP-exposed female cortex and  
389 blood (13 similar DMRs, 1.16% of all DMRs in those tissues), followed by DEHP-exposed male cortex  
390 and blood (10 similar DMRs, 1.12% of all DMRs in those tissues). These findings suggest limited general  
391 overlap in DNAm changes across surrogate and target tissues when stratified by sex and exposure.

392

393 When the similarity of DMR signatures between the sexes was assessed for Pb and DEHP exposures, the  
394 greatest number of shared DMRs was seen in the cortex, followed by blood, with no common DMRs in  
395 the liver (**Figure 2C**). The number of DMRs in common between the sexes did not exceed 2% of the total  
396 DMRs detected in any tissue-exposure combination. These findings highlight the need to evaluate sex-  
397 specific effects in toxicoepigenetic studies.<sup>52,53</sup> A greater degree of DMR similarity was seen between  
398 exposure types, with 1-7% of total DMRs appearing in both Pb and DEHP-exposed tissues, depending on  
399 the sex and tissue (**Figure 2D**). General trends in DMR directionality were not conserved across tissue  
400 types, adding complexity to comparisons of changes in DNAm patterns between target and surrogate  
401 tissues (**Figure 2E**). As expected, many DMRs were located in CpG islands, areas of dynamic DNAm-  
402 directed gene expression regulation.<sup>54</sup> Gene promoters and exons also contained more DMRs than would  
403 have been predicted by chance (**Figure 3**).

404

405 *Exposure-Associated DMRs Occur to a Notable Degree in Imprinted Genes.* An analysis of GO terms  
406 associated with DMR-containing genes identified genomic imprinting as a common category across most  
407 tissues in both sexes and exposure types (**Figures 4 and 5**). Imprinted genes are an important class with  
408 regard to early growth and development, and their epigenetically-controlled mono-allelic parent of origin  
409 nature of expression may confer particular susceptibility to the impacts of environmental exposures.<sup>55,56</sup>  
410 Early disruption of imprinted gene expression and function can result in developmental disorders (e.g.,  
411 pseudohypoparathyroidism type 1B and Silver-Russell syndrome, for which perturbations in gene  
412 expression regulation of *Gnas* and *Grb10*, respectively, have been implicated.<sup>57,58</sup> Additionally, changes  
413 in the DNAm status of several imprinted genes have been associated with chronic conditions such as

414 diabetes, cardiovascular disease, and cancer.<sup>59-61</sup> The DNAm and hydroxymethylation status of imprinted  
415 genes is particularly susceptible to environmental exposures during early development, including Pb and  
416 DEHP.<sup>62-64</sup> Epidemiological studies have linked early life Pb exposure to altered methylation in imprinted  
417 genes including insulin-like growth factor 2 (*IGF2*), which is involved in some cases of Beckwith-  
418 Wiedemann Syndrome and Silver-Russell Syndrome and maternally expressed gene 3 (*MEG3*), which is  
419 implicated in Temple syndrome and Kagami-Ogata syndrome).<sup>65,66</sup>

420  
421 *Imprinting Control Regions Contain Exposure- and Tissue-Specific Changes in DNA Methylation.* ICRs  
422 are environmentally sensitive regulatory regions, and changes to their DNAm status can have  
423 consequences for a cluster of imprinted genes.<sup>67</sup> The ICRs of both *Gnas* and *Grb10* contained numerous  
424 Pb- and DEHP-associated DMRs, with *Gnas* ICR DMRs appearing largely in the cortex and to be more  
425 prevalent with DEHP exposure, while the *Grb10* ICR contained about twice as many Pb-associated  
426 DMRs than DEHP and with much more even distribution across the studied tissues.

427 The *Grb10* ICR contained DMRs across all three tissues examined, with a specific DMR replicated in Pb-  
428 exposed male liver and blood. There was an additional DMR in common in DEHP-exposed male cortex  
429 and blood, but they differed in directionality (cortex = hypomethylated, blood = hypermethylated). The  
430 current study is one the few reports that examine the effects of environmental exposures on the *Grb10*  
431 ICR, with a previous report highlighting the effects on hydroxymethylation,<sup>64</sup> though many more exist  
432 pertaining to changes throughout the gene.<sup>68,69</sup> Much of the published work is restricted to germ cells, and  
433 so additional work is needed to assess whether *Grb10* regulation and function are impacted by the  
434 environment in the soma.

435 *Differential Methylation of Gnas and Grb10 Occurred in Gene Expression Regulatory Regions.* *Gnas*  
436 encodes for the G-protein alpha-subunit protein, which contributes to signal transduction via cAMP  
437 generation<sup>70</sup>, and its imprinting dysregulation has been associated with increased insulin sensitivity,  
438 neural tube defects, and hypothyroidism.<sup>71,72</sup> The imprinted expression of *Gnas* is complex, as this gene  
439 gives rise to several maternal- and paternal-specific gene products, and these patterns of expression are  
440 highly tissue-specific in mice and humans.<sup>73-75</sup> In this work, *Gnas* contained a mix of hyper- and  
441 hypomethylated DMRs in the cortex, under both exposure conditions (**Figure 6**), making the prediction  
442 of the observed sustained DNAm effects at 5 months difficult to ascertain. However, given the  
443 importance of maintained imprinted expression of this locus and its various gene products in the brain,  
444 continued evaluation of the effects of exposure-induced changes in DNAm at this locus would help  
445 elucidate the functional impacts on gene product expression and subsequent physiological effects.  
446 Changes in DNAm within *Gnas* were much more uniform in blood and liver, where biallelic expression is  
447 considered to be the norm in adult mice.<sup>70</sup> Distinct differences in *Gnas* DMR direction appeared between  
448 the sexes in this study (**Figure 6**). In Pb-exposed blood, *Gnas* DMRs were entirely hypomethylated in  
449 males and hypermethylated in females. Within DEHP-exposed blood, *Gnas* DMRs were entirely  
450 hypermethylated in males and a mix of hyper- and hypomethylated in females (**Figure 6**). As this work  
451 found hypomethylation in *Gnas* promoters of DEHP-exposed female cortex and blood, it would be  
452 pertinent to expand this work to additional tissues such as the thyroid to ascertain whether this  
453 relationship is consistent in an organ known to be significantly impacted by developmental changes in  
454 *Gnas* DNAm status.

455 *Grb10* encodes for an insulin receptor-binding protein involved in growth and insulin response and is  
456 imprinted in a tissue- and cell-type specific manner.<sup>76,77</sup> This is especially true during development, as  
457 changes in *Grb10* expression across time are tissue-specific. For example, in the brain, *Grb10* imprinting  
458 status is cell-type specific during development until adulthood.<sup>78</sup> There were several DMRs detected in  
459 *Grb10* in DEHP-exposed male cortex, as well as Pb-exposed male and female cortex. *Grb10* methylation  
460 appears to be cell-type specific during early brain development, with paternal expression in cortical  
461 neurons and maternal expression in glial cells.<sup>77</sup> While this study was unable to assess cell-type specific

462 changes in DNAm within the cortex, future single-cell analyses could help determine whether exposure-  
463 associated DMRs are specific to certain cellular populations. *Grb10* expression also changes significantly  
464 in the liver during development, as maternal expression is high during fetal development, but nearly all  
465 *Grb10* expression is silenced in the liver in adulthood.<sup>79,80</sup> Many of the DMRs seen in *Grb10* in the liver  
466 were hypermethylated, suggesting these exposures may not result in the reactivation of this gene in  
467 adulthood, but, alternatively, may reinforce its suppression through supplemental methylation. Whether  
468 this trend was present during early development, when imprinted expression is the norm and whether that  
469 had any deleterious effects on liver development, remains to be seen. Pb exposure, on the other hand, was  
470 associated with hypomethylation of *Grb10* in female blood, another tissue in which *Grb10* is thought to  
471 be maternally expressed during early development and completely repressed during adulthood,<sup>80</sup> meaning  
472 that exposure may be related to reactivation of this gene during an inappropriate time point. Future  
473 evaluation of the impact of *Grb10* expression in blood during adulthood would contribute to our  
474 understanding of the potential functional impact of this change in methylation. *Grb10* is initially  
475 expressed from the maternal allele in somatic lineages and exclusively in neurons, switches to paternal-  
476 specific expression from an alternate promoter.<sup>77</sup>

477 *Gnas* and *Grb10* Provide Evidence of DNA Methylation Signatures in Target-Surrogate Tissue Pairs. The  
478 ICRs of both *Gnas* and *Grb10* displayed some changes in DNAm that were replicated in both target and  
479 surrogate tissues, suggesting these regulatory regions may be of significance when attempting to identify  
480 DNAm-related biomarkers of exposure (**Figure 7**). Among Pb-exposed samples, the *Grb10* ICR  
481 contained hypermethylated DMRs in male cortex, liver, and blood, suggesting that, for this exposure, the  
482 *Grb10* ICR may be a potential region to consider when exploring male-specific DNAm biomarkers of  
483 exposure. Among DEHP-exposed samples, the *Gnas* ICR contained hyper- and hypomethylated DMRs  
484 that were seen in female cortex and blood, while the *Nespas* ICR was the location of hypermethylated  
485 DMRs in male cortex and blood. These findings suggest there may be ICR- and sex-specificity in terms  
486 of DNAm biomarkers of DEHP exposure, and that they may be particularly applicable to the cortex and  
487 blood. DEHP-associated hypermethylated DMRs were also replicated in male cortex and blood within the  
488 *Grb10* ICR, suggesting this regulatory region may be an additional candidate as a DNAm biomarker for  
489 DEHP exposure.

## 490 **Limitations**

491 DNAm patterns vary across cell types within a given tissue.<sup>81,82</sup> This study was unable to account for cell  
492 type and therefore, changes in DNAm as the result of Pb or DEHP exposure may be due to exposure-  
493 induced changes in cell type proportions.<sup>83</sup> Additionally, we were not able to evaluate changes in DNA  
494 hydroxymethylation (5hmC) in these samples. This study was conducted using bisulfite conversion,  
495 which accounts for both 5mC and 5hmC, and the resulting data is unable to differentiate between these  
496 two signatures.<sup>64</sup> Imprinted genes are typically 50% methylated (accounting for mono-allelic expression  
497 or repression), and this data represents DNAm averages for both alleles. Thus, any allele-specific changes  
498 in DNAm associated with Pb or DEHP cannot be detected.

## 499 **Conclusion**

500 This study systematically evaluated changes in DNAm for cortex, blood, and liver collected from mice at  
501 5 months-of-age following developmental exposure to either Pb or DEHP. Pb- and DEHP-specific  
502 DNAm changes were observed via DMRs, with the greatest DMR similarity seen between exposure  
503 types, with less overlap between the sexes and tissues. Genomic imprinting was impacted by Pb and  
504 DEHP exposure, as determined by GO term analysis, and imprinted genes *Gnas* and *Grb10* indicated  
505 changes in DNAm at their respective ICRs. These results indicate that imprinted gene methylation can be  
506 dysregulated by developmental environmental exposures such as Pb and DEHP and that ICRs may be  
507 useful candidates when exploring DNAm-based biomarkers of environmental exposures.

508 **Acknowledgements**

509 We would like to acknowledge members of the University of Michigan Epigenomics Core and the  
510 Advanced Genomics Core, as well as the Michigan Lifestage Environmental Exposures and Disease  
511 Center (M-LEEd) which facilitated the generation and analysis of WGBS data.

512 **Conflict of Interest**

513 The authors report there are no competing interests to declare.

514 **Funding**

515 This work was supported by funding from the following sources: National Institute of Environmental  
516 Health Sciences (NIEHS) TaRGET II Consortium (ES026697), NIEHS Grant R35 (ES031686), NIEHS  
517 Grant K01 (ES032048), NIEHS Grant R01 (ES028802), the Michigan Lifestage Environmental  
518 Exposures and Disease (M-LEEd) NIEHS Core Center (P30 ES017885), Institutional Training Grant  
519 T32 (ES007062), Institutional Training Grant T32 (HD079342), and National Institute on Aging (NIA)  
520 Grant R01 (AG072396).

521 **Data Sharing**

522 WGBS data will be uploaded to GEO. Additional data that support the findings of this study are available  
523 from the corresponding author, DCD, upon reasonable request.

524

525 **Approval for Animal Use**

526

527 Work outlined in this manuscript was approved by the University of Michigan Institutional Animal Care  
528 and Use Committee (IACUC) and conducted in accordance with the highest animal welfare standards.

529

530

531

532

533

534

535

536

537

538

539

540

541

542 **Figure 1: Overview of experimental workflow.** F0 generation females (6-8 weeks of age) were exposed  
543 to either 32ppm of Pb via drinking water or 5mg/kg-day of DEHP via food, beginning two weeks prior to  
544 mating using virgin males (8-10 weeks of age). Exposure to Pb or DEHP or control continued through  
545 gestation and weaning, when F1 mice were removed from the dams and placed on control water or chow.  
546 At 5 months of age, F1 mice were sacrificed, and genomic DNA was extracted from blood, liver, and  
547 cortex tissues. DNA was used to prepare libraries for Whole Genome Bisulfite Sequencing (WGBS).  
548 Following initial data processing, Differentially Methylated Regions (DMRs) were called using  
549 MethylSig and metilene.

550 **Figure 2: Summary of detected Differentially Methylated Regions.** Differentially Methylated Regions  
551 (DMRs) were categorized by tissue (blood, cortex, and liver), sex (F: female, M: male), and exposure  
552 group (Pb, DEHP, and control) (2A), and DMRs found in more than one tissue type were further  
553 categorized by sex and exposure (2B). DMRs shared by both sexes (2C) and by exposure group (2D)  
554 were quantified and broken down by tissue type. Proportions of DMR directional changes were generally  
555 summarized for each tissue-sex-exposure combination, designated by DNA hyper (more methylated) or  
556 hypo (less methylated), in comparison to controls (2E).

557 **Figure 3: Genomic region of detected Differentially Methylated Regions.** Differentially Methylated  
558 Regions (DMRs) were mapped to the mouse reference genome (mm10) and their genomic region  
559 annotated as percentage of total DMRs (comparing control and exposed samples) for that sex and  
560 exposure within each tissue. This distribution was compared to what would be expected in a random  
561 distribution.

562

563 **Figure 4: GO-terms associated with Differentially Methylated Region-containing genes among Pb-**  
564 **exposed tissues.** Differentially Methylated Region-containing genes found in Pb-exposed tissues were  
565 submitted for Gene Ontology (GO) term analysis across three categories: Biological Process (GOBP),  
566 Cellular Component (GOCC), and Molecular Function (GOMF).

567

568 **Figure 5: GO-terms associated with Differentially Methylated Region-containing genes among**  
569 **DEHP-exposed tissues.** Differentially Methylated Region-containing genes found in DEHP-exposed  
570 tissues were submitted for Gene Ontology (GO) term analysis across three categories: Biological Process  
571 (GOBP), Cellular Component (GOCC), and Molecular Function (GOMF).

572

573 **Figure 6: Genomic location and direction of Pb and DEHP-associated Differentially Methylated**  
574 **Regions in the *Gnas* and *Grb10* loci.** Differentially Methylated Regions (DMRs) detected in the *Gnas*  
575 and *Grb10* loci were classified as to their genomic location within each gene. Percent change in  
576 methylation is denoted by size and direction of methylation change by color (blue = hypermethylated  
577 DMRs among DEHP samples, yellow = hypomethylation among DEHP samples, red = hypermethylation  
578 among Pb samples, green = among hypomethylation among Pb samples).

579

580 **Figure 7: Differentially Methylated Regions detected within *Gnas* and *Grb10* Imprinting Control**  
581 **Regions (ICRs) among Pb and DEHP exposed tissues.** (A) Differentially Methylated Regions (DMRs)  
582 overlap with *Gnas*. (B) DMRs overlap with *Grb10*. DMRs only represents the related genomic locations  
583 corresponding to the genomic coordinates of ICRs. The genomic coordinates of these DMRs can be found  
584 in Supplementary Table 4.

585

586 **References**

- 587 1 Gillman MW. Developmental origins of health and disease. *The New England Journal of*  
588 *Medicine* 2005;**353**:1848.
- 589 2 Bernal AJ, Jirtle RL. Epigenomic disruption: the effects of early developmental exposures. *Birth*  
590 *Defects Research Part A: Clinical and Molecular Teratology* 2010;**88**:938–44.
- 591 3 Bollati V, Baccarelli A. Environmental epigenetics. *Heredity* 2010;**105**:105–12.
- 592 4 Lyko F. The DNA methyltransferase family: a versatile toolkit for epigenetic regulation. *Nature*  
593 *Reviews Genetics* 2018;**19**:81–92.
- 594 5 Siegfried Z, Simon I. DNA methylation and gene expression. *Wiley Interdisciplinary Reviews:*  
595 *Systems Biology and Medicine* 2010;**2**:362–71.
- 596 6 Zeng Y, Chen T. DNA methylation reprogramming during mammalian development. *Genes*  
597 2019;**10**:257.
- 598 7 SanMiguel JM, Bartolomei MS. DNA methylation dynamics of genomic imprinting in mouse  
599 development. *Biol Reprod* 2018;**99**:252–62. <https://doi.org/10.1093/biolre/iroy036>.
- 600 8 Tucci V, Isles AR, Kelsey G, Ferguson-Smith AC, Bartolomei MS, Benvenisty N, *et al.* Genomic  
601 imprinting and physiological processes in mammals. *Cell* 2019;**176**:952–65.
- 602 9 Piedrahita JA. The role of imprinted genes in fetal growth abnormalities. *Birth Defects Res A*  
603 *Clin Mol Teratol* 2011;**91**:682–92. <https://doi.org/10.1002/bdra.20795>.
- 604 10 Moore GE, Ishida M, Demetriou C, Al-Olabi L, Leon LJ, Thomas AC, *et al.* The role and  
605 interaction of imprinted genes in human fetal growth. *Philos Trans R Soc Lond B Biol Sci*  
606 2015;**370**:20140074. <https://doi.org/10.1098/rstb.2014.0074>.
- 607 11 Jima DD, Skaar DA, Planchart A, Motsinger-Reif A, Cevik SE, Park SS, *et al.* Genomic map  
608 of candidate human imprint control regions: the imprintome. *Epigenetics* 2022:1–24.
- 609 12 Horsthemke B. Mechanisms of Imprint Dysregulation.
- 610 13 Faulk C, Dolinoy DC. Timing is everything: the when and how of environmentally induced  
611 changes in the epigenome of animals. *Epigenetics* 2011;**6**:791–7.
- 612 14 Angers B, Castonguay E, Massicotte R. Environmentally induced phenotypes and DNA  
613 methylation: how to deal with unpredictable conditions until the next generation and after.  
614 *Molecular Ecology* 2010;**19**:1283–95.
- 615 15 Senut M-C, Cingolani P, Sen A, Kruger A, Shaik A, Hirsch H, *et al.* Epigenetics of early-life  
616 lead exposure and effects on brain development. *Epigenomics* 2012;**4**:665–74.  
617 <https://doi.org/10.2217/epi.12.58>.
- 618 16 Parsanathan R, Karundevi B. Phthalate exposure in utero causes epigenetic changes and  
619 impairs insulin signalling. *Journal of Endocrinology* 2014;**223**:47–66.  
620 <https://doi.org/10.1530/JOE-14-0111>.
- 621 17 Dignam T, Kaufmann RB, LeStourgeon L, Brown MJ. Control of Lead Sources in the  
622 United States, 1970-2017: Public Health Progress and Current Challenges to Eliminating Lead  
623 Exposure. *J Public Health Manag Pract* 2019;**25**:S13–22.  
624 <https://doi.org/10.1097/PHH.0000000000000889>.
- 625 18 Zhou F, Yin G, Gao Y, Liu D, Xie J, Ouyang L, *et al.* Toxicity assessment due to prenatal  
626 and lactational exposure to lead, cadmium and mercury mixtures. *Environ Int*  
627 2019;**133**:105192. <https://doi.org/10.1016/j.envint.2019.105192>.

- 628 19 Kamenov GD, Swarngen BF, Cornwell DA, McTigue NE, Roberts SM, Bonzongo J-CJ.  
629 High-precision Pb isotopes of drinking water lead pipes: Implications for human exposure to  
630 industrial Pb in the United States. *Sci Total Environ* 2023;**871**:162067.  
631 <https://doi.org/10.1016/j.scitotenv.2023.162067>.
- 632 20 Dietrich M, Barlow CF, Entwistle JA, Meza-Figueroa D, Dong C, Gunkel-Grillon P, *et al*.  
633 Predictive modeling of indoor dust lead concentrations: Sources, risks, and benefits of  
634 intervention. *Environ Pollut* 2023;**319**:121039. <https://doi.org/10.1016/j.envpol.2023.121039>.
- 635 21 Wang Y, Qian H. Phthalates and Their Impacts on Human Health. *Healthcare (Basel)*  
636 2021;**9**:603. <https://doi.org/10.3390/healthcare9050603>.
- 637 22 Lin Y, Wei J, Li Y, Chen J, Zhou Z, Song L, *et al*. Developmental exposure to di(2-  
638 ethylhexyl) phthalate impairs endocrine pancreas and leads to long-term adverse effects on  
639 glucose homeostasis in the rat. *American Journal of Physiology-Endocrinology and Metabolism*  
640 2011;**301**:E527–38. <https://doi.org/10.1152/ajpendo.00233.2011>.
- 641 23 Erythropel HC, Maric M, Nicell JA, Leask RL, Yargeau V. Leaching of the plasticizer di(2-  
642 ethylhexyl)phthalate (DEHP) from plastic containers and the question of human exposure.  
643 *Appl Microbiol Biotechnol* 2014;**98**:9967–81. <https://doi.org/10.1007/s00253-014-6183-8>.
- 644 24 Wang T, Pehrsson EC, Purushotham D, Li D, Zhuo X, Zhang B, *et al*. The NIEHS TaRGET II  
645 Consortium and environmental epigenomics. *Nature Biotechnology* 2018;**36**:225–7.
- 646 25 Dou JF, Farooqui Z, Faulk CD, Barks AK, Jones T, Dolinoy DC, *et al*. Perinatal Lead (Pb)  
647 Exposure and Cortical Neuron-Specific DNA Methylation in Male Mice. *Genes (Basel)*  
648 2019;**10**:E274. <https://doi.org/10.3390/genes10040274>.
- 649 26 Faulk C, Barks A, Liu K, Goodrich JM, Dolinoy DC. Early-life lead exposure results in dose-  
650 and sex-specific effects on weight and epigenetic gene regulation in weanling mice.  
651 *Epigenomics* 2013;**5**:487–500. <https://doi.org/10.2217/epi.13.49>.
- 652 27 Schmidt J-S, Schaedlich K, Fiandanese N, Pocar P, Fischer B. Effects of di(2-ethylhexyl)  
653 phthalate (DEHP) on female fertility and adipogenesis in C3H/N mice. *Environ Health Perspect*  
654 2012;**120**:1123–9. <https://doi.org/10.1289/ehp.1104016>.
- 655 28 Neier K, Cheatham D, Bedrosian LD, Dolinoy DC. Perinatal exposures to phthalates and  
656 phthalate mixtures result in sex-specific effects on body weight, organ weights and  
657 intracisternal A-particle (IAP) DNA methylation in weanling mice. *J Dev Orig Health Dis*  
658 2019;**10**:176–87. <https://doi.org/10.1017/S2040174418000430>.
- 659 29 Percie du Sert N, Hurst V, Ahluwalia A, Alam S, Avey MT, Baker M, *et al*. The ARRIVE  
660 guidelines 2.0: Updated guidelines for reporting animal research. *PLoS Biol* 2020;**18**:e3000410.  
661 <https://doi.org/10.1371/journal.pbio.3000410>.
- 662 30 Svoboda LK, Neier K, Wang K, Cavalcante RG, Rygiel CA, Tsai Z, *et al*. Tissue and sex-  
663 specific programming of dna methylation by perinatal lead exposure: implications for  
664 environmental epigenetics studies. *Epigenetics* 2021;**16**:1102–22.  
665 <https://doi.org/10.1080/15592294.2020.1841872>.
- 666 31 Andrews. *FastQC A Quality Control tool for High Throughput Sequence Data*. 2010. URL:  
667 <https://www.bioinformatics.babraham.ac.uk/projects/fastqc/> (Accessed 15 February 2023).
- 668 32 Ewels P, Magnusson M, Lundin S, Källér M. MultiQC: summarize analysis results for  
669 multiple tools and samples in a single report. *Bioinformatics* 2016;**32**:3047–8.  
670 <https://doi.org/10.1093/bioinformatics/btw354>.

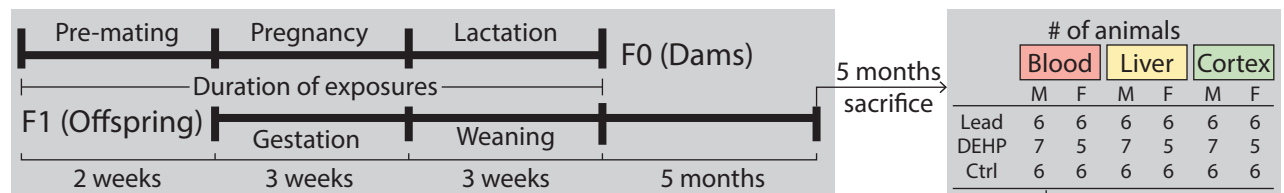
- 671 33 Krueger F. *Trim Galore*. 2015. URL:  
672 [https://www.bioinformatics.babraham.ac.uk/projects/trim\\_galore/](https://www.bioinformatics.babraham.ac.uk/projects/trim_galore/) (Accessed 15 February  
673 2023).
- 674 34 Krueger F, Andrews SR. Bismark: a flexible aligner and methylation caller for Bisulfite-  
675 Seq applications. *Bioinformatics* 2011;**27**:1571–2.  
676 <https://doi.org/10.1093/bioinformatics/btr167>.
- 677 35 Langmead B, Salzberg SL. Fast gapped-read alignment with Bowtie 2. *Nat Methods*  
678 2012;**9**:357–9. <https://doi.org/10.1038/nmeth.1923>.
- 679 36 Jühling F, Kretzmer H, Bernhart SH, Otto C, Stadler PF, Hoffmann S. metilene: fast and  
680 sensitive calling of differentially methylated regions from bisulfite sequencing data. *Genome*  
681 *Res* 2016;**26**:256–62. <https://doi.org/10.1101/gr.196394.115>.
- 682 37 Park Y, Figueroa ME, Rozek LS, Sartor MA. MethylSig: a whole genome DNA methylation  
683 analysis pipeline. *Bioinformatics* 2014;**30**:2414–22.  
684 <https://doi.org/10.1093/bioinformatics/btu339>.
- 685 38 Cavalcante RG, Sartor MA. annotatr: genomic regions in context. *Bioinformatics*  
686 2017;**33**:2381–3. <https://doi.org/10.1093/bioinformatics/btx183>.
- 687 39 Welch RP, Lee C, Imbriano PM, Patil S, Weymouth TE, Smith RA, *et al*. ChIP-Enrich: gene  
688 set enrichment testing for ChIP-seq data. *Nucleic Acids Res* 2014;**42**:e105.  
689 <https://doi.org/10.1093/nar/gku463>.
- 690 40 Williamson CM, Blake A, Thomas S, Beechey CV, Hancock J, Cattanach BM, *et al*. World  
691 Wide Web Site-Mouse Imprinting Data and References. *Oxfordshire: MRC Hartwell* 2013.
- 692 41 Tucci V, Isles AR, Kelsey G, Ferguson-Smith AC, Tucci V, Bartolomei MS, *et al*. Genomic  
693 Imprinting and Physiological Processes in Mammals. *Cell* 2019;**176**:952–65.  
694 <https://doi.org/10.1016/j.cell.2019.01.043>.
- 695 42 Juan AM, Foong YH, Thorvaldsen JL, Lan Y, Leu NA, Rurik JG, *et al*. Tissue-specific  
696 Grb10/Ddc insulator drives allelic architecture for cardiac development. *Mol Cell*  
697 2022;**82**:3613–3631.e7. <https://doi.org/10.1016/j.molcel.2022.08.021>.
- 698 43 Wang L, Zhang J, Duan J, Gao X, Zhu W, Lu X, *et al*. Programming and inheritance of  
699 parental DNA methylomes in mammals. *Cell* 2014;**157**:979–91.  
700 <https://doi.org/10.1016/j.cell.2014.04.017>.
- 701 44 Riemondy KA, Sheridan RM, Gillen A, Yu Y, Bennett CG, Hesselberth JR. valr:  
702 Reproducible genome interval analysis in R. *F1000Res* 2017;**6**:1025.  
703 <https://doi.org/10.12688/f1000research.11997.1>.
- 704 45 Dolinoy DC, Weidman JR, Jirtle RL. Epigenetic gene regulation: linking early  
705 developmental environment to adult disease. *Reprod Toxicol* 2007;**23**:297–307.  
706 <https://doi.org/10.1016/j.reprotox.2006.08.012>.
- 707 46 Thomason ME, Hect JL, Rauh VA, Trentacosta C, Wheelock MD, Eggebrecht AT, *et al*.  
708 Prenatal lead exposure impacts cross-hemispheric and long-range connectivity in the human  
709 fetal brain. *Neuroimage* 2019;**191**:186–92.  
710 <https://doi.org/10.1016/j.neuroimage.2019.02.017>.
- 711 47 Neier K, Montrose L, Chen K, Malloy MA, Jones TR, Svoboda LK, *et al*. Short- and long-  
712 term effects of perinatal phthalate exposures on metabolic pathways in the mouse liver.  
713 *Environ Epigenet* 2020;**6**:dvaa017. <https://doi.org/10.1093/eep/dvaa017>.



- 714 48 Rygiel CA, Goodrich JM, Solano-González M, Mercado-García A, Hu H, Téllez-Rojo MM,  
715 *et al.* Prenatal Lead (Pb) Exposure and Peripheral Blood DNA Methylation (5mC) and  
716 Hydroxymethylation (5hmC) in Mexican Adolescents from the ELEMENT Birth Cohort. *Environ*  
717 *Health Perspect* 2021;**129**:67002. <https://doi.org/10.1289/EHP8507>.
- 718 49 Chen C-H, Jiang SS, Chang I-S, Wen H-J, Sun C-W, Wang S-L. Association between fetal  
719 exposure to phthalate endocrine disruptor and genome-wide DNA methylation at birth.  
720 *Environ Res* 2018;**162**:261–70. <https://doi.org/10.1016/j.envres.2018.01.009>.
- 721 50 Sobolewski M, Varma G, Adams B, Anderson DW, Schneider JS, Cory-Slechta DA.  
722 Developmental Lead Exposure and Prenatal Stress Result in Sex-Specific Reprogramming of  
723 Adult Stress Physiology and Epigenetic Profiles in Brain. *Toxicol Sci* 2018;**163**:478–89.  
724 <https://doi.org/10.1093/toxsci/kfy046>.
- 725 51 Liu S, Wang K, Svoboda LK, Rygiel CA, Neier K, Jones TR, *et al.* Perinatal DEHP exposure  
726 induces sex- and tissue-specific DNA methylation changes in both juvenile and adult mice.  
727 *Environ Epigenet* 2021;**7**:dvab004. <https://doi.org/10.1093/eep/dvab004>.
- 728 52 Svoboda LK, Ishikawa T, Dolinoy DC. Developmental toxicant exposures and sex-specific  
729 effects on epigenetic programming and cardiovascular health across generations. *Environ*  
730 *Epigenet* 2022;**8**:dvac017. <https://doi.org/10.1093/eep/dvac017>.
- 731 53 Singh G, Singh V, Sobolewski M, Cory-Slechta DA, Schneider JS. Sex-Dependent Effects of  
732 Developmental Lead Exposure on the Brain. *Front Genet* 2018;**9**:89.  
733 <https://doi.org/10.3389/fgene.2018.00089>.
- 734 54 Smallwood SA, Tomizawa S-I, Krueger F, Ruf N, Carli N, Segonds-Pichon A, *et al.* Dynamic  
735 CpG island methylation landscape in oocytes and preimplantation embryos. *Nat Genet*  
736 2011;**43**:811–4. <https://doi.org/10.1038/ng.864>.
- 737 55 Kang E-R, Iqbal K, Tran DA, Rivas GE, Singh P, Pfeifer GP, *et al.* Effects of endocrine  
738 disruptors on imprinted gene expression in the mouse embryo. *Epigenetics* 2011;**6**:937–50.  
739 <https://doi.org/10.4161/epi.6.7.16067>.
- 740 56 Krishnamoorthy M, Gerwe BA, Scharer CD, Heimbürg-Molinari J, Gregory F, Nash RJ, *et*  
741 *al.* GABRB3 gene expression increases upon ethanol exposure in human embryonic stem cells.  
742 *J Recept Signal Transduct Res* 2011;**31**:206–13.  
743 <https://doi.org/10.3109/10799893.2011.569723>.
- 744 57 Bastepe M, Fröhlich LF, Hendy GN, Indridason OS, Josse RG, Koshiyama H, *et al.*  
745 Autosomal dominant pseudohypoparathyroidism type 1b is associated with a heterozygous  
746 microdeletion that likely disrupts a putative imprinting control element of *GNAS*. *J Clin Invest*  
747 2003;**112**:1255–63. <https://doi.org/10.1172/JCI19159>.
- 748 58 Eggermann T, Begemann M, Kurth I, Elbracht M. Contribution of GRB10 to the prenatal  
749 phenotype in Silver-Russell syndrome? Lessons from 7p12 copy number variations. *Eur J Med*  
750 *Genet* 2019;**62**:103671. <https://doi.org/10.1016/j.ejmg.2019.103671>.
- 751 59 Wallace C, Smyth DJ, Maisuria-Armer M, Walker NM, Todd JA, Clayton DG. The  
752 imprinted DLK1-MEG3 gene region on chromosome 14q32.2 alters susceptibility to type 1  
753 diabetes. *Nat Genet* 2010;**42**:68–71. <https://doi.org/10.1038/ng.493>.
- 754 60 Tahara S, Tahara T, Horiguchi N, Okubo M, Terada T, Yoshida D, *et al.* Lower LINE-1  
755 methylation is associated with promoter hypermethylation and distinct molecular features in  
756 gastric cancer. *Epigenomics* 2019;**11**:1651–9. <https://doi.org/10.2217/epi-2019-0091>.

- 757 61 Ito Y, Koessler T, Ibrahim AEK, Rai S, Vowler SL, Abu-Amero S, *et al.* Somatically acquired  
758 hypomethylation of IGF2 in breast and colorectal cancer. *Hum Mol Genet* 2008;**17**:2633–43.  
759 <https://doi.org/10.1093/hmg/ddn163>.
- 760 62 Nye MD, King KE, Darrah TH, Maguire R, Jima DD, Huang Z, *et al.* Maternal blood lead  
761 concentrations, DNA methylation of MEG3 DMR regulating the DLK1/MEG3 imprinted domain  
762 and early growth in a multiethnic cohort. *Environ Epigenet* 2016;**2**:dvv009.  
763 <https://doi.org/10.1093/eep/dvv009>.
- 764 63 Li L, Zhang T, Qin X-S, Ge W, Ma H-G, Sun L-L, *et al.* Exposure to diethylhexyl phthalate  
765 (DEHP) results in a heritable modification of imprint genes DNA methylation in mouse  
766 oocytes. *Mol Biol Rep* 2014;**41**:1227–35. <https://doi.org/10.1007/s11033-013-2967-7>.
- 767 64 Kochmanski JJ, Marchlewicz EH, Cavalcante RG, Perera BPU, Sartor MA, Dolinoy DC.  
768 Longitudinal Effects of Developmental Bisphenol A Exposure on Epigenome-Wide DNA  
769 Hydroxymethylation at Imprinted Loci in Mouse Blood. *Environmental Health Perspectives*  
770 n.d.;**126**:077006. <https://doi.org/10.1289/EHP3441>.
- 771 65 Kalish JM, Jiang C, Bartolomei MS. Epigenetics and imprinting in human disease. *Int J*  
772 *Dev Biol* 2014;**58**:291–8. <https://doi.org/10.1387/ijdb.140077mb>.
- 773 66 Prasasya R, Grotheer KV, Siracusa LD, Bartolomei MS. Temple syndrome and Kagami-  
774 Ogata syndrome: clinical presentations, genotypes, models and mechanisms. *Hum Mol Genet*  
775 2020;**29**:R107–16. <https://doi.org/10.1093/hmg/ddaa133>.
- 776 67 Doshi T, D'souza C, Vanage G. Aberrant DNA methylation at Igf2-H19 imprinting control  
777 region in spermatozoa upon neonatal exposure to bisphenol A and its association with post  
778 implantation loss. *Mol Biol Rep* 2013;**40**:4747–57. [https://doi.org/10.1007/s11033-013-2571-](https://doi.org/10.1007/s11033-013-2571-x)  
779 [x](https://doi.org/10.1007/s11033-013-2571-x).
- 780 68 Schrott R, Greeson KW, King D, Symosko Crow KM, Easley CA, Murphy SK. Cannabis  
781 alters DNA methylation at maternally imprinted and autism candidate genes in spermatogenic  
782 cells. *Syst Biol Reprod Med* 2022;**68**:357–69.  
783 <https://doi.org/10.1080/19396368.2022.2073292>.
- 784 69 Soubry A, Hoyo C, Butt CM, Fieuws S, Price TM, Murphy SK, *et al.* Human exposure to  
785 flame-retardants is associated with aberrant DNA methylation at imprinted genes in sperm.  
786 *Environmental Epigenetics* 2017;**3**:dvx003. <https://doi.org/10.1093/eep/dvx003>.
- 787 70 Weinstein LS, Xie T, Zhang Q-H, Chen M. Studies of the regulation and function of the  
788 Gsa gene Gnas using gene targeting technology. *Pharmacol Ther* 2007;**115**:271–91.  
789 <https://doi.org/10.1016/j.pharmthera.2007.03.013>.
- 790 71 Wang L, Chang S, Wang Z, Wang S, Huo J, Ding G, *et al.* Altered GNAS imprinting due to  
791 folic acid deficiency contributes to poor embryo development and may lead to neural tube  
792 defects. *Oncotarget* 2017;**8**:110797–810. <https://doi.org/10.18632/oncotarget.22731>.
- 793 72 Hanna P, Francou B, Delemer B, Jüppner H, Linglart A. A Novel Familial PHP1B Variant  
794 With Incomplete Loss of Methylation at GNAS-A/B and Enhanced Methylation at GNAS-AS2. *J*  
795 *Clin Endocrinol Metab* 2021;**106**:2779–87. <https://doi.org/10.1210/clinem/dgab136>.
- 796 73 Turan S, Bastepe M. The GNAS complex locus and human diseases associated with loss-  
797 of-function mutations or epimutations within this imprinted gene. *Horm Res Paediatr*  
798 2013;**80**:10.1159/000355384. <https://doi.org/10.1159/000355384>.

- 799 74 Wroe SF, Kelsey G, Skinner JA, Bodle D, Ball ST, Beechey CV, *et al.* An imprinted  
800 transcript, antisense to Nesp, adds complexity to the cluster of imprinted genes at the mouse  
801 Gnas locus. *Proc Natl Acad Sci U S A* 2000;**97**:3342–6. <https://doi.org/10.1073/pnas.97.7.3342>.
- 802 75 Hayward BE, Kamiya M, Strain L, Moran V, Campbell R, Hayashizaki Y, *et al.* The human  
803 GNAS1 gene is imprinted and encodes distinct paternally and biallelically expressed G  
804 proteins. *Proc Natl Acad Sci U S A* 1998;**95**:10038–43.  
805 <https://doi.org/10.1073/pnas.95.17.10038>.
- 806 76 Desbuquois B, Carré N, Burnol A-F. Regulation of insulin and type 1 insulin-like growth  
807 factor signaling and action by the Grb10/14 and SH2B1/B2 adaptor proteins. *FEBS J*  
808 2013;**280**:794–816. <https://doi.org/10.1111/febs.12080>.
- 809 77 Plasschaert RN, Bartolomei MS. Tissue-specific regulation and function of Grb10 during  
810 growth and neuronal commitment. *Proc Natl Acad Sci U S A* 2015;**112**:6841–7.  
811 <https://doi.org/10.1073/pnas.1411254111>.
- 812 78 Hikichi T, Kohda T, Kaneko-Ishino T, Ishino F. Imprinting regulation of the murine  
813 Meg1/Grb10 and human GRB10 genes; roles of brain-specific promoters and mouse-specific  
814 CTCF-binding sites. *Nucleic Acids Res* 2003;**31**:1398–406. <https://doi.org/10.1093/nar/gkg232>.
- 815 79 Luo L, Jiang W, Liu H, Bu J, Tang P, Du C, *et al.* De-silencing Grb10 contributes to acute  
816 ER stress-induced steatosis in mouse liver. *J Mol Endocrinol* 2018;**60**:285–97.  
817 <https://doi.org/10.1530/JME-18-0018>.
- 818 80 Blagitko N, Mergenthaler S, Schulz U, Wollmann HA, Craigen W, Eggermann T, *et al.*  
819 Human GRB10 is imprinted and expressed from the paternal and maternal allele in a highly  
820 tissue- and isoform-specific fashion. *Human Molecular Genetics* 2000;**9**:1587–95.  
821 <https://doi.org/10.1093/hmg/9.11.1587>.
- 822 81 Bakulski KM, Feinberg JL, Andrews SV, Yang J, Brown S, L. McKenney S, *et al.* DNA  
823 methylation of cord blood cell types: Applications for mixed cell birth studies. *Epigenetics*  
824 2016;**11**:354–62. <https://doi.org/10.1080/15592294.2016.1161875>.
- 825 82 Armand EJ, Li J, Xie F, Luo C, Mukamel EA. Single-Cell Sequencing of Brain Cell  
826 Transcriptomes and Epigenomes. *Neuron* 2021;**109**:11–26.  
827 <https://doi.org/10.1016/j.neuron.2020.12.010>.
- 828 83 Campbell KA, Colacino JA, Park SK, Bakulski KM. Cell types in environmental epigenetic  
829 studies: Biological and epidemiological frameworks. *Curr Environ Health Rep* 2020;**7**:185–97.  
830 <https://doi.org/10.1007/s40572-020-00287-0>.
- 831



Genomic DNA/RNA from tissues  
+  
Library preparation for WGBS

Illumina NovaSeq 6000

Quality control (FastQC & MultiQC) + Trimming (trim\_galore)  
Alignment (bowtie2) + CpG methylation calls (Bismark)

### MethylSig

- Filter out CpGs by coverage ( $10 < cov < 500$ )
- Filter out CpGs with reads covered in less than 4 samples per group; Define tiling windows 100 bps
- Select regions with  $FDR < 0.15$  and methylation difference  $> 5\%$

### DMRs

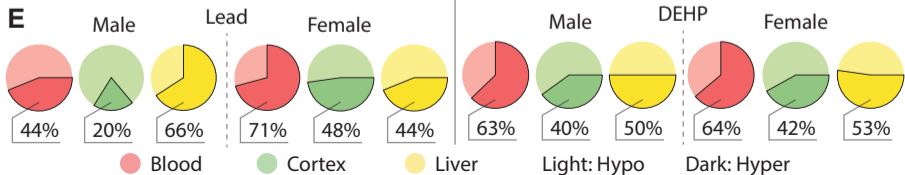
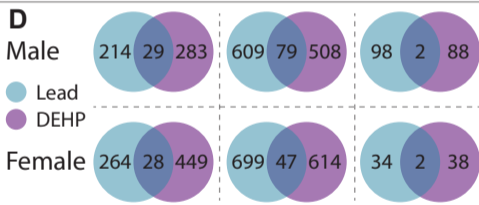
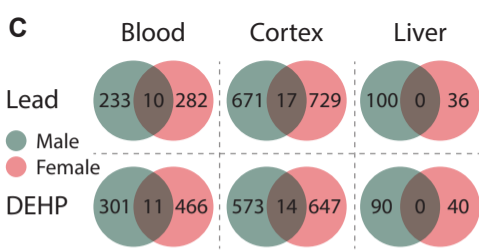
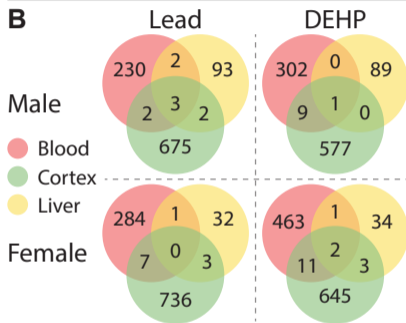
- Combine DMRs from MethylSig and metilene for downstream analysis
- Any overlapped DMRs will be merged together as one DMR

### metilene

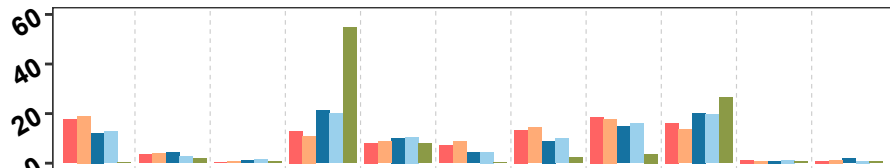
- Filter out CpGs by coverage ( $10 < cov < 500$ )
- Generate input data with metilene\_input.pl
- Run metilene with  $\geq 5$  CpGs in a DMR
- Select regions with  $FDR < 0.15$  and methylation difference  $> 5\%$

**A**

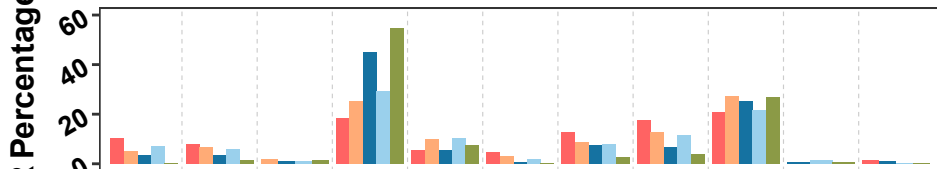
	Blood		Cortex		Liver	
	M	F	M	F	M	F
lead	243	292	688	746	100	36
DEHP	312	477	587	661	90	40



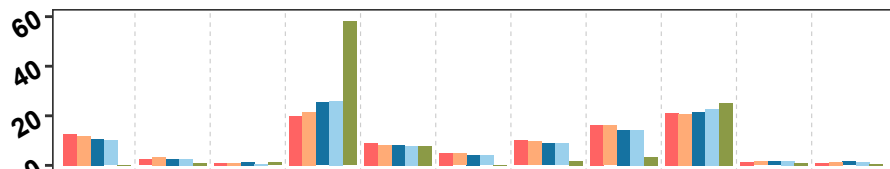
### Blood



### Liver

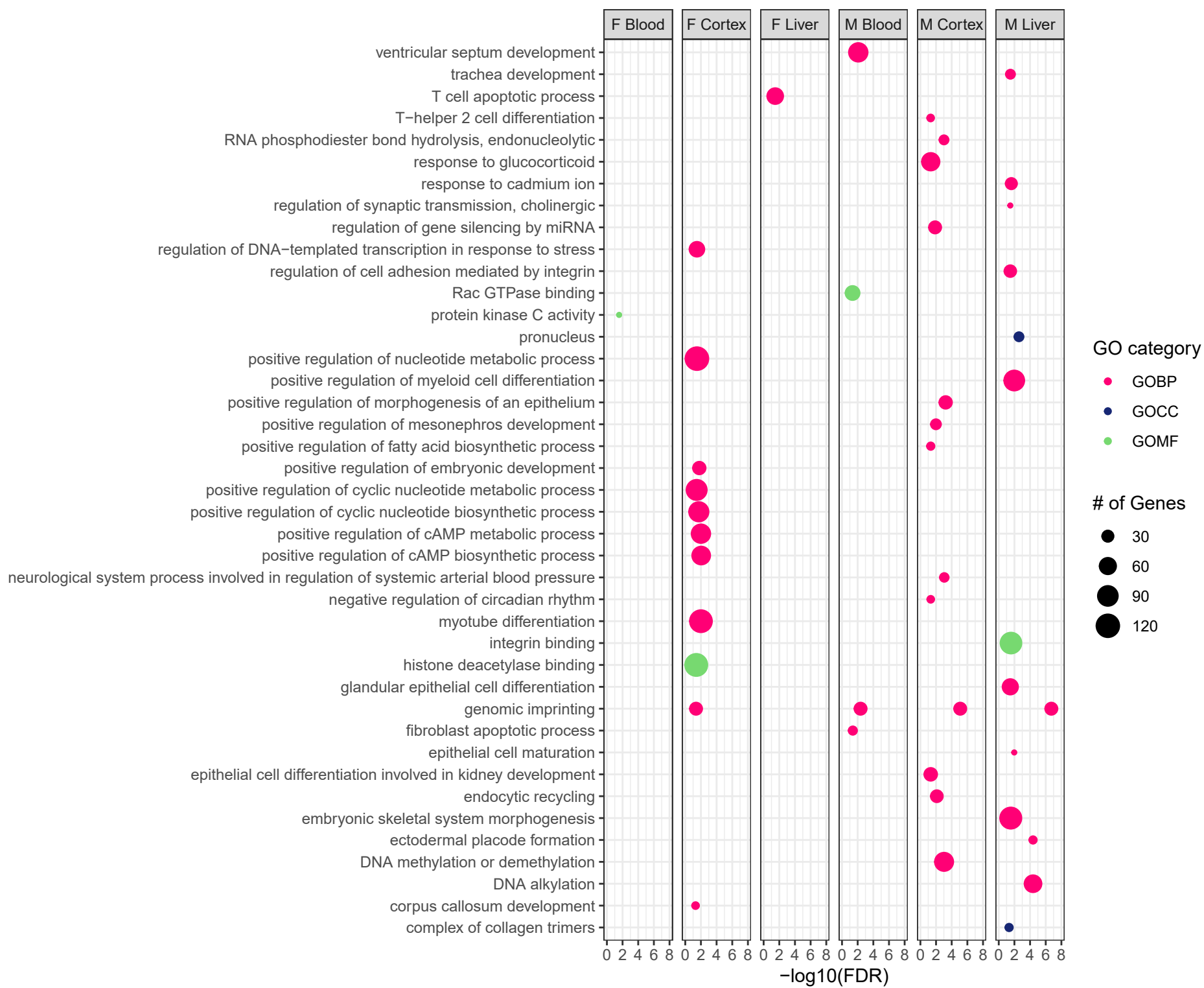


### Cortex



### Genomic Region

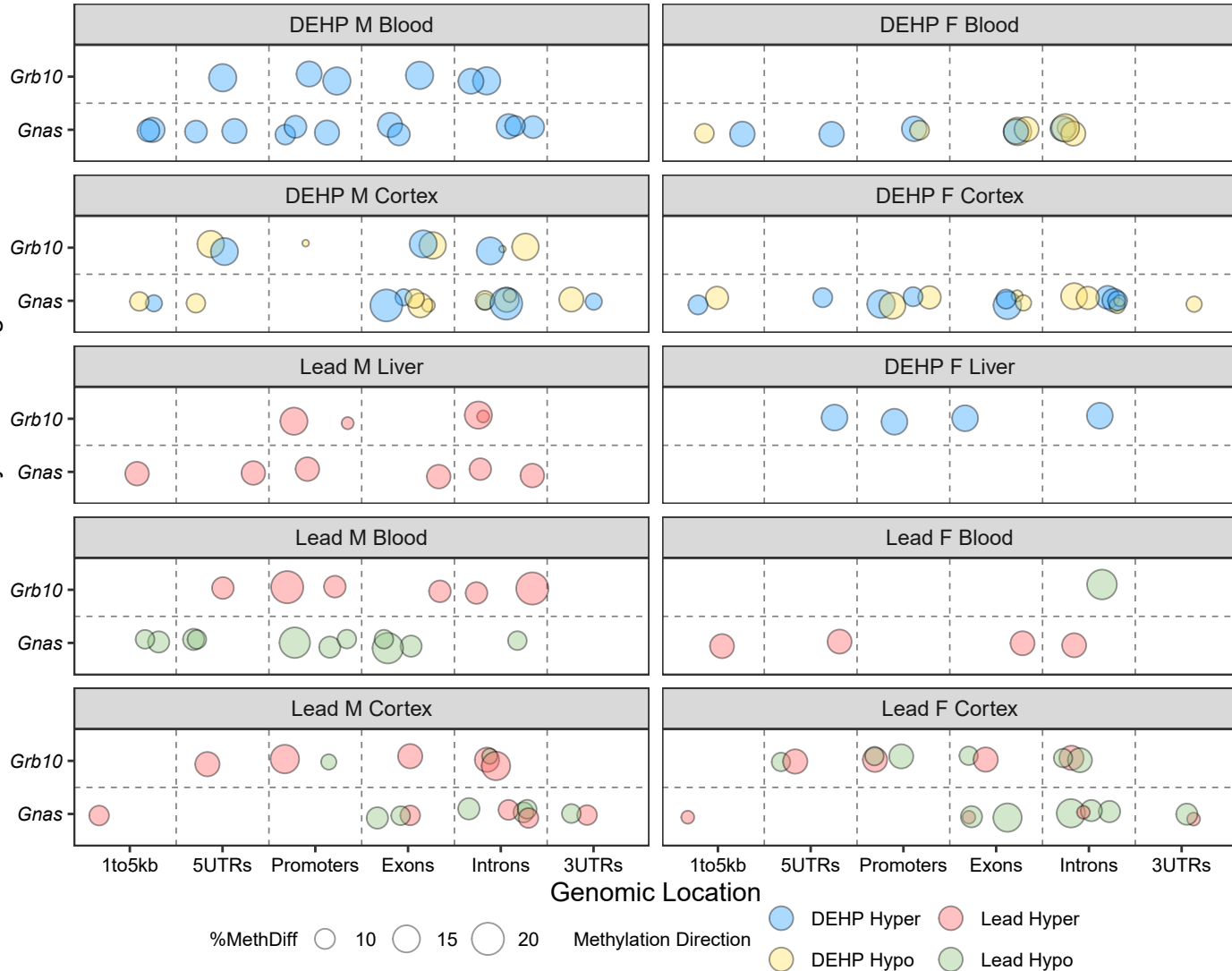








DNA Methylation Changes



%MethDiff ○ 10 ○ 15 ○ 20

Methylation Direction

- DEHP Hyper
- Lead Hyper
- DEHP Hypo
- Lead Hypo

